Few-electron systems in quantum cylinders

B. Szafran, J. Adamowski, and S. Bednarek
Faculty of Physics and Nuclear Techniques, University of Mining and Metallurgy (AGH), Kraków, Poland
(Received 10 August 1999)

Systems of excess electrons confined in cylindrical semiconductor quantum dots, i.e., artificial atoms of cylindrical symmetry, are studied by the unrestricted Hartree-Fock method. The confinement potential is assumed in the form of three-dimensional cylindrically symmetric potential well of finite depth. The calculations have been performed for artificial atoms with the number of electrons from 1 to 10. We have taken into account the external magnetic field applied parallel to the axis of the cylinder and studied the influence of quantum-dot geometry on the maximum number of confined electrons and the ground-state spinorbital configuration. The applicability of the quasi-two-dimensional model of quantum dots has been discussed and the magnetic-field behavior has been predicted for quantum cylinders of comparable diameter and height. We have applied the present model to a description of single-electron charging of self-assembled quantum dots and obtained a good agreement with capacitance-spectroscopy data.

I. INTRODUCTION

In semiconductor quantum dots,[1] the charge carriers are confined in all three dimensions. The confinement potential results from either different compositions of semiconducting materials of the dot and the surrounding medium or the electrostatic potential applied to the microelectrodes. Many-electron systems confined in quantum dots exhibit atomlike properties and are called artificial atoms.[2] A discrete energy spectrum of artificial atoms is observed in absorption measurements.[3] Shell-filling effects are observed in capacitance[4] and transport spectroscopy.[5]

Nowadays, the quantum dots of cylindrical symmetry are the subject of extensive experimental and theoretical investigations. These are the self-assembled quantum dots[6–11] or gate-controlled quantum dots.[12–16] In theoretical papers[7–11] on electron systems in self-assembled quantum dots, various confinement potentials have been used. The confinement potential of finite depth was used for one-electron problem in a lens-shape[8] or pyramidal self-assembled quantum dot[9,10] grown on a thin wetting layer. Many-electron problem for these potentials has not been solved so far. A qualitative description of the *N*-electron systems confined in self-assembled quantum dots has been obtained[7] within a two-dimensional parabolic potential model. A recent paper[11] showed, however, that this model potential does not allow for a quantitative description of the single-electron charging experiment.[6] In order to obtain a quantitative agreement with the capacitance-spectroscopy data,[6] the authors[11] were forced to decouple two intrinsically coupled parameters, namely, the oscillator energy and oscillator length, and treat them as two independent adjustable parameters. A pronounced breaking of the generalized Kohn theorem[2,17] observed in the far-infrared absorption spectrum of InAs self-assembled quantum dots,[18] suggests that the confining potential of the quantum dots differs significantly from the harmonic-oscillator form. The applicability of the two-dimensional model for quantum dots is usually justified by a large energy separation between the ground-state and first excited-state energy level of the size quantized motion in the *z* direction. In the present paper, we discuss the limitation of this model and obtain conditions under which this model fails.

In our recent papers,[19,20] we have presented a theoretical description of electron systems confined in spherical quantum dots, i.e., artificial atoms of spherical symmetry. In the present paper, we extend the previous theory[19,20] to systems of lower symmetry, i.e., electrons in cylindrical quantum dots with the confinement potential well of finite depth. Since the experiments on electron properties of cylindrical quantum dots are usually done in external magnetic field,[4,6,12,13] which gives information about the strength of electron localization and symmetries of the observed states, in the present paper we take into account the effect of this field. We have applied the present approach to a description of single-electron charging of self-assembled quantum dots.[6]

In this paper, we present a consistent quantitative theory of the single-electron charging experiment.[6] The present theoretical description of the self-assembled quantum dots is fully three dimensional. The applied model confinement potential takes into account the conduction-band offset between the dot region and surrounding material. Therefore, the present approach is free of the following shortcomings of the two-dimensional harmonic-oscillator model: (i) a strictly planar movement of interacting electrons has to be assumed (ii) this confinement potential does not possess a definite range, which means that the localization radius of the confined-electron system rapidly grows with the number of electrons; (iii) this model potential possesses an infinite depth and can bind an infinite number of electrons; (iv) the three-dimensional Coulomb interaction is inadequately described[21] by the strictly two-dimensional model.

In contrast to (ii), the electrons confined in the three-dimensional potential well of finite depth are spread out over the entire quantum-dot volume with only a small penetration into the barrier region. In this case, the localization radius of electron system is almost independent of the number of electrons. The Schrödinger equation for the potential well of finite depth possesses not only bound but also unbound (delocalized) solutions, i.e., the continuum threshold exists. Therefore, in the frame of this model, we can discuss a maxi-

mum number of confined electrons and the quantum capacity[19,20] of the nanostructure.

The paper is organized as follows: in Sec. II, we present the theoretical model, in Sec. III, we apply this model to a description of self-assembled quantum dots, in Sec. IV, we discuss the influence of geometry of the confinement on the electronic properties of quantum dots, and in Sec. V we provide the conclusions.

II. THEORY

The effective-mass Hamiltonian of N excess electrons confined in a cylindrical quantum dot in the presence of external magnetic field applied parallel to the z axis of the cylinder has the form

$$\mathcal{H}=\sum_{i=1}^{N} h(\mathbf{r}_i)+\frac{1}{4\pi\varepsilon\varepsilon_0}\sum_{i=1}^{N}\sum_{j>i}^{N}\frac{1}{r_{ij}}, \tag{1}$$

where $h(\mathbf{r}_i)$ is the one-electron Hamiltonian

$$h(\mathbf{r})=-\frac{\hbar^2}{2m^*}\nabla^2+V(\mathbf{r})+\frac{1}{8}m^*\omega_c^2(x^2+y^2)+\frac{1}{2}\hbar\omega_c l_z. \tag{2}$$

Here, m^* is the electron effective band mass, ε is the static dielectric constant of the quantum dot material, $\omega_c=eB/m^*$ is the cyclotron frequency in magnetic field B, and l_z is the z -component angular momentum operator. The confinement potential of the cylindrical quantum dot of diameter D and height H is taken on in the form

$$V(\mathbf{r})=\begin{cases}-V_0, & \text{if } \sqrt{x^2+y^2}<D/2 \text{ and } |z|<H/2,\\ 0, & \text{otherwise,}\end{cases} \tag{3}$$

where $V_0>0$ is the conduction-band discontinuity at the quantum well/barrier interface. The conduction-band minimum of the barrier material in the absence of external magnetic field is set equal to zero and taken as the reference energy level. We neglect the change of effective mass and dielectric constant at the well/barrier surface.[19,22]

Let us remind the basic properties of the one-electron Hamiltonian (2). Due to the cylindrical symmetry of the confinement potential, one-electron Hamiltonian (2) commutes with l_z operator and the operator of reflection with respect to the $z=0$ plane. Therefore, we can assign to the one-electron eigenstates of Hamiltonian (2) the magnetic quantum number M, i.e., the eigenvalue of l_z operator, and the parity quantum number. In the absence of external magnetic field the states with $M=0$ are twofold degenerate, the other states are fourfold degenerate. The interaction of an electron with the external magnetic field is included in the last two terms of Hamiltonian (2). The third term leads to an increased localization of an electron in the $x-y$ plane. The fourth lifts the degeneracy of states with different signs of the magnetic quantum number. In the present paper, we neglect the spin Zeeman effect, which in the III-V semiconducting compounds is two orders of magnitude smaller than the orbital Zeeman effect.[13]

The Schrödinger equation for the N-electron system has been solved by the unrestricted Hartree-Fock method. The many-electron wave function is constructed in the form of a single Slater determinant of one-electron spinorbitals. The Slater determinant built from the one-electron wave functions of the proper symmetry is an eigenfunction of the z component of total angular momentum and has a definite z parity. The one-electron Hartree-Fock operator[23] conserves the symmetry of Hamiltonian (2).

The spatial one-electron wave function ψ has been expanded[24] into the Gaussian variational basis as follows:

$$\psi(x,y,z)=\sum_{klmpq} c_{klmpq}x^k y^l z^m e^{-\alpha_p(x^2+y^2)-\beta_q z^2}, \tag{4}$$

where the sums over k and l run from 0 to $k+l\leqslant 2$, $m=0,1$, and $p,q=1,2$. c_{klmpq}, α_p, and β_q are the variational parameters. The nonlinear parameters α_p and β_q account for the electron localization in the $x-y$ plane and z direction respectively, and are optimized to yield the minimum value of the total energy. The linear variational parameters c_{klmpq} for all the occupied spin orbitals are obtained by the self-consistent iterative diagonalization of the Hartree-Fock equations. In our previous papers,[19,22] we discussed the applicability of the Slater and Gaussian bases to the problem of one particle confined in the finite quantum well. The Gaussian basis cannot reproduce the discontinuity of the second derivative of the exact wave function on the well/barrier surface.[25] However, as we have shown,[22] the variational cost of this discrepancy is small. Basis (4) possesses the proper cylindrical symmetry and yields accurate estimates of the lowest one-electron energy levels corresponding to $M=0,\pm 1,\pm 2$. In the present calculations, we take into account the lowest-energy state of even parity and the lowest-energy state of odd parity for the quantized motion in the z direction. Throughout the present paper, we denote the one-electron states as follows: $a_{n_z,\pm}$, where $a=s,p,d$ for $|M|=0,1,2$, respectively, the quantum number n_z labels the states associated with the size-quantized motion in the z direction ($n_z=0$ for the state of even parity and $n_z=1$ for the state of odd parity), and $\pm$ stands for the sign of M.

The unrestricted Hartree-Fock method was used by several authors[19,26–28] to a description of artificial atoms. The properties of electron systems in quantum dots were also studied with the correlation effects included by the configuration-interaction approach[2,14,15,29–31] and density-functional theory.[16,32,33] We have shown in our previous papers[19,20] that in the case of spherically symmetric potential well of finite depth, the Hartree-Fock method yields reliable solutions of the many-electron Schrödinger equation in the strong- and intermediate-confinement regimes,[34] i.e., if the range of the confinement potential does not exceed $\sim$10 donor Bohr radii (i.e., $\sim$100 nm for GaAs). This condition is fulfilled in the case of self-assembled quantum dots, that have a base length of order of 10-30 nm.[6,18,35–38] We can therefore expect that the neglect of electron-electron correlation is justified for these systems.

III. SINGLE-ELECTRON CHARGING OF SELF-ASSEMBLED QUANTUM DOTS

We have applied the present model to a theoretical description of the capacitance-spectroscopy experiment with self-assembled InAs/GaAs quantum dots.[6] The samples[6]

were fabricated by a molecular-beam epitaxy and InAs quantum dots were grown in a Stranski-Krastanow growth mode[36] on a GaAs substrate. The quantum dots[6] were almost uniform in size (within 10-percent fluctuations) with average diameter 20 nm and height 7 nm. The layer sequence[6] consisted of a Si-doped GaAs back contact, undoped GaAs tunnel barrier, InAs wetting layer with InAs self-assembled quantum dots, undoped GaAs layer, blocking barrier (made of GaAs/AlAs superlattice), and GaAs cap layer with a Schottky gate contact. The number of excess electrons per dot was tuned with the voltage applied between the gate and back contact.[6] In the measurements of capacitance-voltage characteristics,[6] the Nth peak of capacitance was detected at the gate voltage for which the Fermi level of the back contact and the chemical potential of N excess electrons confined in the quantum dot were aligned. The condition of the single-electron charging has the form

$$E_F = \mu_N^0 + e\lambda(V_S - V_g), \tag{5}$$

where μ_N^0 is the chemical potential of the N-electron system confined in the dot in the absence of external electric field, V_g is the gate voltage, V_S is the Schottky barrier between the metal gate and semiconductor, e is the elementary charge, and λ is the voltage-to-energy conversion coefficient. We have taken on $V_S = 650$ meV according to Ref. 40 and the value $\lambda = 1/7$ deduced from the geometrical position of the dot layer with respect to the electrodes.[6,11] The change of electrostatic potential inside the dot has been neglected in Eq. (5), which is justified by the small height of the dot. The Fermi energy of the doped GaAs back contact is fixed at the position of the donor energy level. The variation of the Fermi level in the external magnetic field calculated by the first-order perturbation theory can be expressed as $E_F = E_D + 8.28\,[\mathrm{meV/T^2}] \times 10^{-3} B^2$, where $E_D = -6$ meV is the donor energy. The chemical potential has been determined as follows: $\mu_N^0 = E_N - E_{N-1}$, where E_N is the ground-state energy of the N-electron artificial atom.

Since the parameters of the quantum dots are not known with the required precision, in the present calculations, the diameter D and height H of the cylinder, the depth of the potential well V_0, and dielectric constant ε of the dot material have been adjusted to reproduce all the experimentally measured V_g vs B plots.[6] The best results have been obtained for $D = 22$ nm, $H = 6.3$ nm, $V_0 = 317$ meV, and $\varepsilon = 13.5$. Moreover, the value of the electron effective band mass for the strained InAs dot has been taken from Refs. 6 and 11 ($m_e = 0.057 m_{e0}$, where m_{e0} is the free-electron rest mass). Such a procedure allows us to account partially for the strain effects[9] and alloying of the quantum dots material due to the diffusion of indium atoms after the GaAs overgrowth.[39]

The calculated gate voltage corresponding to the capacitance peaks for $N = 1, \ldots, 8$ electrons is plotted in Fig. 1 as a function of the magnetic field B and compared with the results of the capacitance spectroscopy.[6] The magnetic field lifts the degeneracy of states with the quantum numbers M and $-M$, which gives rise to a change of symmetry of the N-electron ground state at certain critical magnetic fields (marked by arrows in Fig. 1). The critical fields B_1 and B_6 correspond to a magnetic-field-induced breaking of Hund's rule in the 4- and 8-electron artificial atoms, respectively.

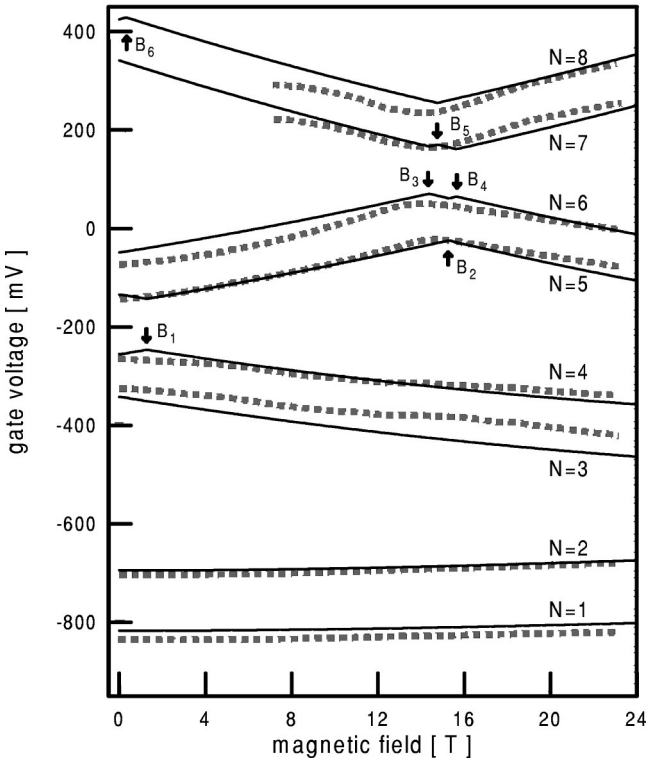

FIG. 1. Calculated (solid curves) and measured (squares) gate voltage, which corresponds to the charging of the quantum dot by the Nth electron, as a function of magnetic field. Arrows show critical magnetic fields $B_1, \ldots, B_6$, at which the N-electron ground-state configuration changes (see text and Table I).

The cusp corresponding to the breaking of Hund's rule in 4-electron artificial atom (B_1) is not clearly visible in the experimental data[6] because of significant inhomogeneous broadening resulting from the size distribution of quantum dots. However, this feature has been clearly observed in transport spectroscopy of gated quantum dots.[12,13] The critical magnetic fields giving rise to the breaking of the Hund's rule cannot be described with the use of local-density-approximation approach,[16] which does not resolve spin and replace the exchange operator by its local approximation.

If the magnetic field exceeds critical values $B_2, \ldots, B_5$, then in the 5-, 6-, and 7-electron artificial atoms, the one-electron $d_{0,-}$ spinorbitals become occupied and the $p_{0,+}$ spinorbitals become empty. These ground-state transformations are explained in detail in Table I, in which we list the estimated critical magnetic fields and electron configurations before and after the transformation. Figure 1 shows that the calculated positions of the capacitance peaks on the gate-voltage scale agree very well with the experimental data.[6]

IV. INFLUENCE OF QUANTUM DOT GEOMETRY ON THE PROPERTIES OF CONFINED ELECTRON SYSTEMS

Having at our disposal the theoretical method, which leads to the very good agreement with experiment, we have solved by this method the problem of the influence of nanostructure geometry on the properties of electrons confined in cylindrical quantum dots. In Fig. 2, we report the results for the lowest-energy levels of a single electron in the cylindrical quantum dot in the absence of magnetic field. The values

TABLE I. Estimated critical magnetic fields B_i (in tesla), for which the transformation of N-electron ground state occurs. The values of parameters of the quantum dot are the same as in Fig. 1. The occupation of one-electron spinorbitals and quantum numbers (M_{tot},S_{tot}), where M_{tot} corresponds to the z component of total angular momentum and S_{tot} – the z-component of total spin, are listed for $B \leqslant B_i (B > B_i)$ in the fourth and fifth (sixth and seventh) columns. For all the spinorbitals $n_z = 0$ and this index is omitted.

B_i	[T]	N	$B \leqslant B_i$		$B > B_i$	
B_1	1.25	4	$s^2 p_- p_+$	(0,1)	$s^2 p_-^2$	$(-2,0)$
B_2	15.3	5	$s^2 p_-^2 p_+$	$(-1,\frac{1}{2})$	$s^2 p_-^2 d_-$	$(-4,\frac{1}{2})$
B_3	14.4	6	$s^2 p_-^2 p_+^2$	(0,0)	$s^2 p_-^2 p_+ d_-$	$(-3,1)$
B_4	15.6	6	$s^2 p_-^2 p_+ d_-$	$(-3,1)$	$s^2 p_-^2 d_-^2$	$(-6,0)$
B_5	14.8	7	$s^2 p_-^2 p_+^2 d_-$	$(-2,\frac{1}{2})$	$s^2 p_-^2 p_+ d_+^2$	$(-5,\frac{1}{2})$
B_6	0.25	8	$s^2 p_-^2 p_+^2 d_- d_+$	(0,1)	$s^2 p_-^2 p_+^2 d_-^2$	$(-4,0)$

of all the material parameters are the same as in Fig. 1. We see that the increase of the cylinder height more strongly affects the states with $n_z = 1$ than those with $n_z = 0$. In particular, the s_1 energy level, which corresponds to the state of odd parity, becomes lower than the energy levels of d_0 and p_0 states, if the height of the dot exceeds 12 nm and 19.5 nm, respectively. In Fig. 3, we have plotted the chemical potentials for $N = 1, \ldots, 10$ electrons as functions of the cylinder height (the values of material parameters are the same as in Figs. 1 and 2). The one-electron levels occupied by the Nth electron are marked in the figure. The kinks in the curves result from the changes of the ground-state configuration due to the crossing of one-electron energy levels presented in Fig. 2.

Using the results shown in Fig. 3, we have estimated the

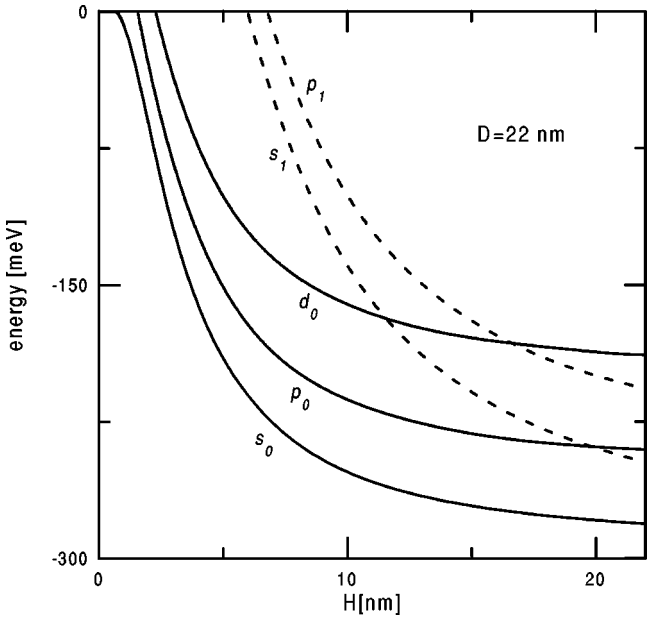

FIG. 2. Energy levels of the single electron confined in the cylindrical quantum dot of diamater $D = 22$ nm in the absence of external magnetic field as functions of height H of the dot. Solid (dashed) curves display the results for the states with $n_z = 0 (n_z = 1)$. The sign of M is not shown, since the energy levels corresponding to $\pm M$ are degenerate.

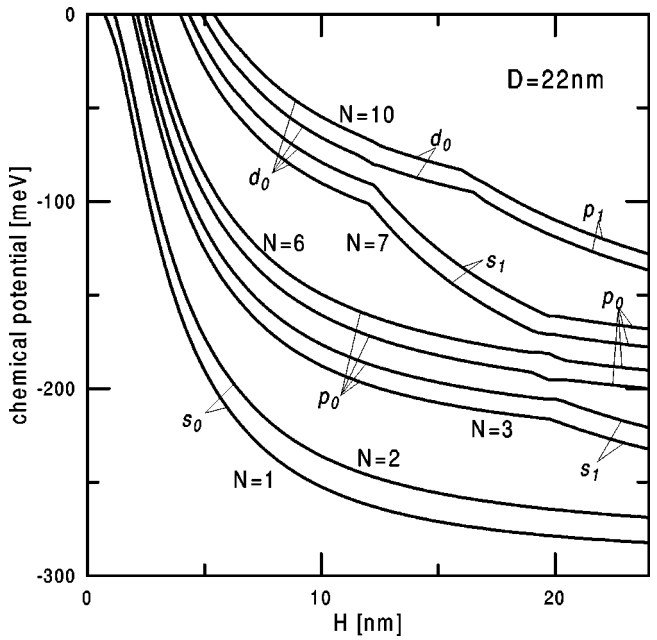

FIG. 3. Chemical potentials of N-electron systems confined in a cylindrical quantum dot of diameter $D = 22$ nm as functions of its height H. Symbols denote the one-electron orbitals occupied by the Nth electron. The kinks on the curves correspond to the changes of the ground-state symmetry.

maximum number of electrons confined in the cylindrical quantum dot. The N-electron system can form a bound state in the quantum dot if[19,20]

$$E_N < E_{N-1}. \tag{6}$$

This condition of binding can be expressed in terms of chemical potential as follows:

$$\mu_N < 0. \tag{7}$$

The values of critical heights of the quantum cylinder, above which the binding of subsequent electrons is possible, have been listed in Table II. In particular we have obtained the result that 10 electrons can be bound in the cylinder of height $H = 6.3$ nm and diameter $D = 22$ nm, which correspond to the self-assembled quantum-dot nanostructure studied in Ref 6. In the experiment,[6] only 8 capacitance peaks have been resolved. Moreover, at low-magnetic fields the charging of the dot with 7th and 8th electron is masked by the strong capacitance signal resulting from the charging of the wetting layer[6] and only 6 single-electron charging lines are clearly visible. Because the added 7th and 8th electrons occupy the d_{0-} shell (cf. Table I), the chemical potentials of 7- and 8-electron artificial atoms decrease with the magnetic field and the corresponding capacitance peaks emerge from the

TABLE II. Critical heights of cylindrical quantum dot, above which the binding of N electrons is possible. Parameters of the quantum dot are the same as in Fig. 1 ($D = 22$ nm, $V_0 = 317$ meV, $\varepsilon = 13.5$, $m_e = 0.057\ m_0$)

N	1	2	3	4	5	6	7	8	9	10
H [nm]	0.725	1.2	1.9	2.15	2.5	2.75	3.9	4.35	4.9	5.4

strong wetting-layer background at $B\sim 7$ T. The chemical potentials for $N=9$ and $N=10$ electron-systems, for which the d_{0+} shell is filled, increase with increasing magnetic field. Therefore, the corresponding capacitance peaks stay within the range of the wetting layer charging and are not observed. On the other hand, the binding of 9 and 10 electrons in the self-assembled quantum dots[6] predicted by the present quantum-cylinder model may result from the neglect of the presence of wetting layer in the confinement potential (3). The inclusion of the wetting-layer confinement potential in many-electron calculations should clear up the problem of the exact maximum number of electrons confined in self-assembled quantum dots.

The geometry of the nanostructure determines the symmetry of the ground state of many-electron systems confined in the quantum dots. If the range of vertical confinement is much smaller than the lateral one (cf. results of Fig. 1 for $H=6.3$ nm and $D=22$ nm), the separations between the energy levels corresponding to the states with different parity are much larger than those between the energy levels with different magnetic quantum number. In such a case, all the occupied one-electron levels correspond to the lowest-energy state of even parity ($n_z=0$). For the small height of the cylinder ($H<12$ nm) the relative positions of chemical potentials exhibit the filling of shells[12,14,19] of a quasi-two-dimensional confinement potential. In the absence of external magnetic field, the electrons occupy subsequent energy levels according to Hund's rule, i.e., 2 electrons fill the s shell (M=0), 6 electrons the p shell ($M=\pm 1$) and 10 electrons the d shell ($M=\pm 2$). The large difference between μ_2 and μ_3 (μ_6 and μ_7) in Fig. 3 corresponds to the fully filled s_0 (p_0) shell. The visible increments of spacings between μ_4 and μ_5 as well as between μ_8 and μ_9 are signatures of Hund's rule and correspond to the half-filled p_0 and d_0 shells, respectively. The ground-state configurations of the electron artificial atoms with $N=1,\ldots,10$ remain the same up to $H=12$ nm (cf. Fig. 3).

For $H>12$ nm, the levels of odd z parity become occupied and the symmetry of the N-electron ground state changes; therefore the artificial atom looses the quasi-two-dimensional character. In this case, the reaction of the artificial atom to the external magnetic field is essentially different. In Fig. 4, we have presented the magnetic-field dependence of one-electron energy levels (dashed curves) and N-electron chemical potentials (solid curves) of $N=1,\ldots,8$ artificial atoms in a cylindrical quantum well of height $H=18$ nm and diameter $D=22$ nm. The critical fields of the ground-state transformations of the ground state have been marked by arrows. The behavior of chemical potentials for $N=1,\ldots,4$ is qualitatively the same as in Fig. 1. The magnetic field B_1 at which the Hund's rule for 4-electron artificial atom is broken, is slightly smaller for $H=22$ nm than for $H=6.3$ nm, because in the case of large dots the electron-electron interactions are weaker. The magnetic-field dependence of chemical potentials for $N=5,\ldots,8$ is different than that for $H=6.3$ nm, because the new orbital s_1 affects the spectrum. The new cusps at critical fields $B_2,\ldots,B_5$ result from the change of order of $p_{0,+}$ and s_1 energy levels. These critical fields do not appear in the quasi-two-dimensional case. The critical fields B_6,B_7, and

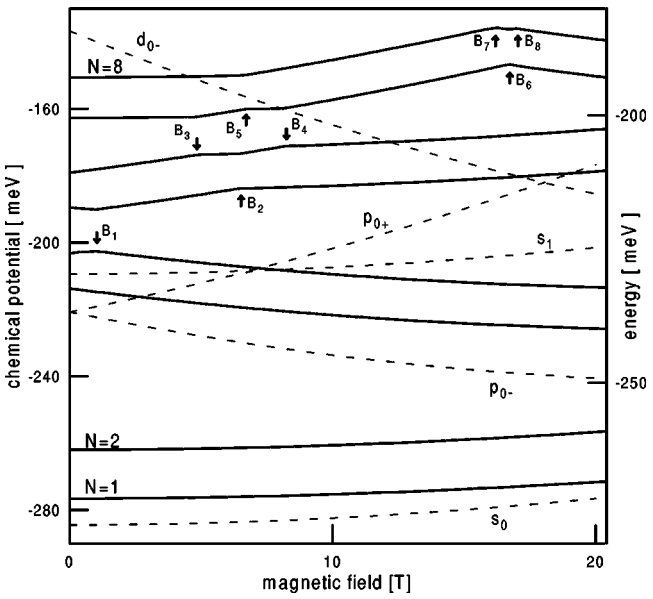

FIG. 4. Chemical potential (solid curves, left scale) for $N=1,\ldots,8$ electrons and one-electron energy levels (dashed curves, right scale) for the cylindrical quantum dot with 18-nm height and 22-nm diameter as functions of magnetic field. The arrows correspond to the ground-state transformations, described in the text and quoted in Table III.

B_8 for $N=7$ and 8 result from the change of order of $p_{0,+}$ and $d_{0,-}$ energy levels. The effect of crossing of these levels has already appeared for flat quantum dots, but for $N=5$ and $N=6$ electrons (cf. critical fields B_2,B_3, and B_4 in Fig. 1). The ground-state transformations are listed in detail in Table III. To the best of our knowledge, we have presented the first results of magnetic field-influence on the N-electron quantum dots beyond the quasi-two-dimensional limit.

The shape of the self-assembled quantum dots[6] can be approximated by the cylinder of rather small height. In the gated quantum dots[12–15] the disproportion between the diameter and height of the dot is even larger. However, the

TABLE III. Estimated critical magnetic fields B_i (in tesla), for which the transformation of N-electron ground state occurs. The values of material parameters are the same as in Fig. 4. The occupation of one-electron spinorbitals and quantum numbers (M_{tot},S_{tot}), where M_{tot} corresponds to the z component of total angular momentum and S_{tot} – the z component of total spin, are listed for $B\leqslant B_i$ ($B>B_i$) in the fourth and fifth (sixth and seventh) columns. For s_1 spinorbital $n_z=1$, and for all other spinorbitals $n_z=0$ and this index is omitted.

B_i	[T]	N	$B\leqslant B_i$		$B>B_i$	
B_1	1	4	$s^2p_-p_+$	(0,1)	$s^2p_-^2$	$(-2,0)$
B_2	6.5	5	$s^2p_-^2p_+$	$(-1,\frac{1}{2})$	$s^2p_-^2s_1$	$(-2,\frac{1}{2})$
B_3	4.9	6	$s^2p_-^2p_+^2$	(0,0)	$s^2p_-^2p_+s_1$	$(-1,1)$
B_4	8.2	6	$s^2p_-^2p_+s_1$	$(-1,1)$	$s^2p_-^2s_1^2$	$(-2,0)$
B_5	6.8	7	$s^2p_-^2p_+^2s_1$	$(0,\frac{1}{2})$	$s^2p_-^2p_+s_1^2$	$(-1,\frac{1}{2})$
B_6	16.6	7	$s^2p_-^2p_+s_1^2$	$(-1,\frac{1}{2})$	$s^2p_-^2s_1^2d_-$	$(-4,\frac{1}{2})$
B_7	16.2	8	$s^2p_-^2p_+^2s_1^2$	(0,0)	$s^2p_-^2p_+s_1^2d_-$	$(-3,1)$
B_8	17.1	8	$s^2p_-^2p_+s_1^2d_-$	$(-3,1)$	$s^2p_-^2s_1^2d_-^2$	$(-6,0)$

present technology enables a fabrication of quantum dots of almost arbitrary shapes.[41] Therefore, the present extension of the theory of artificial atoms to the confinement potentials with comparable range in all the three dimensions should be useful for future experiments.

V. CONCLUSION

We have presented a theory of electronic properties of cylindrical quantum dots using the unrestricted Hartree-Fock method and a confinement potential in the form of the finite potential well of cylindrical symmetry. The present theoretical model has been successfully applied to the single-electron charging of self-assembled quantum dots in external magnetic field.[6] We have discussed the influence of the nanostructure geometry on the spin-orbital configurations of the confined N-electron system. The maximum number of electrons, that can be bound in the cylindrical quantum dots, have been determined. In a future study, the wetting layer should be included in the calculations in order to clear up the question of binding of $N=9$ and $N=10$ electron systems in self-assembled quantum dots. We have discussed the applicability of the quasi-two-dimensional model and predicted the magnetic-field dependence of chemical potentials for quantum dots of comparable diameter and height. These results should be useful for quantum dots of new geometries.

ACKNOWLEDGMENT

This paper has been partially supported by the Scientific Research Committee (KBN) under Grant No. 2 P03B 3416.

[1] For review articles, see T. Chakraborty, Comments Condens. Matter Phys. **16**, 35 (1992); M.A. Kastner, Phys. Today **46(1)**, 24 (1993); A.D. Yoffe, Adv. Phys. **42**, 173 (1993); N.F. Johnson, J. Phys.: Condens. Matter **7**, 965 (1995); M.A. Kastner, Comments Condens. Matter Phys. **17**, 349 (1996).

[2] P.A. Maksym, and T. Chakraborty, Phys. Rev. Lett. **65**, 108 (1990).

[3] Ch. Sikorski and U. Merkt, Phys. Rev. Lett. **62**, 2164 (1989).

[4] R.C. Ashoori, H.L. Stormer, J.S. Weiner, L.N. Pfeiffer, S.J. Pearton, K.W. Baldwin, and K.W. West, Phys. Rev. Lett. **68**, 3088 (1992); R.C. Ashoori, H.L. Stormer, J.S. Weiner, L.N. Pfeiffer, K.W. Baldwin, and K.W. West, *ibid.* **71**, 613 (1993).

[5] P.L. McEuen, E.B. Foxman, U. Meirav, M.A. Kastner, Y. Meir, N.S. Wingreen, and S.J. Wind, Phys. Rev. Lett. **66**, 1926 (1991); J. Weis, R.J. Haug, K.v. Klitzing, and K. Ploog, *ibid.* **71**, 4019 (1993).

[6] B.T. Miller, W. Hansen, S. Manus, R.J. Luyken, A. Lorke, J.P. Kotthaus, S. Huant, G. Medeiros-Ribeiro, and P.M. Petroff, Phys. Rev. B **56**, 6764 (1997).

[7] A. Wójs and P. Hawrylak, Phys. Rev. B **53**, 10 841 (1996).

[8] A. Wójs, P. Hawrylak, S. Fafard, and L. Jacak, Phys. Rev. B **54**, 5604 (1996).

[9] M. Grundmann, O. Stier, and D. Bimberg, Phys. Rev. B **52**, 11 969 (1995).

[10] M.A. Cusack, P.R. Briddon, and M. Jaros, Phys. Rev. B **54**, 2300 (1996).

[11] R.J. Warburton, B.T. Miller, C.S. Dürr, C. Bödefeld, K. Karrai, J.P. Kotthaus, G. Medeiros-Ribeiro, P.M. Petroff, and S. Huant, Phys. Rev. B **58**, 16 221 (1998).

[12] S. Tarucha, D.G. Austing, T. Honda, R.J. van der Hage, and L.P. Kouwenhoven, Phys. Rev. Lett. **77**, 3613 (1996).

[13] L.P. Kouwenhoven, T.H. Oosterkamp, M.W.S. Danoesastro, M. Eto, D.G. Austing, T. Honda, and S. Tarucha, Science **278**, 1788 (1997).

[14] M. Eto, J. Appl. Phys. **36**, 3924 (1997).

[15] T. Ezaki, N. Mori, and C. Hamaguchi, Phys. Rev. B **56**, 6428 (1997).

[16] O. Steffens, M. Suhrke, and U. Rössler, Physica B **256-258**, 147 (1998).

[17] P. Bakshi, D.A. Broido, and K. Kempa, Phys. Rev. B **42**, 7416 (1990).

[18] M. Fricke, A. Lorke, J.P. Kotthaus, G. Medeiros-Ribeiro, and P.M. Petroff, Europhys. Lett. **36**, 197 (1996).

[19] S. Bednarek, B. Szafran, and J. Adamowski, Phys. Rev. B **59**, 13 036 (1999).

[20] B. Szafran, J. Adamowski, and S. Bednarek, Physica E **4**, 1 (1999).

[21] M. Rontani, F. Rossi, F. Manghi, and E. Molinari, Phys. Rev. B **59**, 10 165 (1999).

[22] B. Szafran, J. Adamowski, and B. Stébé, J. Phys.: Condens. Matter **10**, 7575 (1998).

[23] J.C. Slater, *Quantum Theory of Atomic Structure* (McGraw-Hill, New York, 1960).

[24] C.C.J. Roothan, Rev. Mod. Phys. **23**, 69 (1951).

[25] S. Flügge and H. Marschall, *Rechenmethoden der Quantentheorie* (Springer Verlag, Berlin, 1952).

[26] M. Fujito, A. Natori, and H. Yasunaga, Phys. Rev. B **53**, 9952 (1996).

[27] J.J. Palacios, L. Martin-Moreno, G. Chiappe, E. Louis, and C. Tejedor, Phys. Rev. B **50**, 5760 (1994).

[28] A. Natori, and D. Nakamura, Jpn. J. Appl. Phys., Part 1 **38**, 380 (1990).

[29] G.W. Bryant, Phys. Rev. Lett. **59**, 1140 (1987).

[30] D. Pfannkuche and R.R Gerhardts, Phys. Rev. B **44**, 13 132 (1991).

[31] U. Merkt, J. Huser, and M. Wagner, Phys. Rev. B **43**, 7320 (1991).

[32] M. Koskinen, M. Manninen, and S.M. Reimann, Phys. Rev. Lett. **79**, 1389 (1997).

[33] K. Hirose and N.S. Wingreen, Phys. Rev. B **59**, 4604 (1999).

[34] L. Banyai and S.W. Koch, *Semiconductor Quantum Dots* (World Scientific, Singapore, 1993).

[35] M. Grundmann, J. Christen, N.N. Ledentsov, J. Böhrer, D. Bimberg, S.S. Ruvimov, P. Werner, U. Richet, U. Gösele, J. Heydenreich, V.M. Ustinov, A.Yu. Egorov, A.E. Zhukov, P.S. Kop'ev, and Zh.I. Alferov, Phys. Rev. Lett. **74**, 4043 (1995).

[36] G. Medeiros-Ribeiro, D. Leonard, and P.M. Petroff, Appl. Phys. Lett. **66**, 1767 (1995).

[37] M.J. Steer, D.J. Mowbray, W.R. Tribe, M.S. Skolnick, M.D. Sturge, M. Hopkinson, A.G. Cullis, C.R. Whitehouse, and R. Murray, Phys. Rev. B **54**, 17 738 (1996).

[38] H. Drexler, D. Leonard, W. Hansen, J.P. Kotthaus, and P.M. Petroff, Phys. Rev. Lett. **73**, 2252 (1994).

[39] P.D. Siverns, S. Malik, G. McPherson, D. Childs, C. Roberts, R. Murray, B.A. Joyce, and H. Davock, Phys. Rev. B **58**, R10 127 (1998).

[40] R.J. Luyken, A. Lorke, M. Haslinger, B.T. Miller, M. Fricke, J.P. Kotthaus, G. Medeiros-Ribeiro, and P.M. Petroff, Physica E **2**, 704 (1998).

[41] L. Pfeiffer, K.W. West, H.L. Stormer, J.P. Eisenstein, K.W. Baldwin, D. Gershoni, and J. Spector, Appl. Phys. Lett. **56**, 1697 (1990).